

9-1-2018

CRISPR-Cas9 Mediated Epitope Tagging Provides Accurate and Versatile Assessment of Myocardin–Brief Report

Qing Lyu

Vidhi Dhagia
New York Medical College

Yu Han

Bing Guo

Mary E. Wines-Samuelsan

See next page for additional authors

Follow this and additional works at: https://touro scholar.touro.edu/nymc_fac_pubs



Part of the [Medicine and Health Sciences Commons](#)

Recommended Citation

Lyu, Q., Dhagia, V., Han, Y., Guo, B., Wines-Samuelsan, M., Christie, C., Yin, Q., Slivano, O., Herring, P., Long, X., Gupte, S., & Miano, J. (2018). CRISPR-Cas9 Mediated Epitope Tagging Provides Accurate and Versatile Assessment of Myocardin–Brief Report. *Arteriosclerosis, Thrombosis, and Vascular Biology*, 38 (9), 2184-2190. <https://doi.org/10.1161/ATVBAHA.118.311171>

This Article is brought to you for free and open access by the Faculty at Touro Scholar. It has been accepted for inclusion in NYMC Faculty Publications by an authorized administrator of Touro Scholar. For more information, please contact touro.scholar@touro.edu.

Authors

Qing Lyu, Vidhi Dhagia, Yu Han, Bing Guo, Mary E. Wines-Samuels, Christine K. Christie, Qiangzong Yin, Orazio J. Slivano, Paul Herring, Xiaochun Long, Sachin A. Gupte, and Joseph M. Miano

CRISPR-Cas9–Mediated Epitope Tagging Provides Accurate and Versatile Assessment of Myocardin—Brief Report

Qing Lyu, Vidhi Dhagia, Yu Han, Bing Guo, Mary E. Wines-Samuelson, Christine K. Christie, Qiangzong Yin, Orazio J. Slivano, Paul Herring, Xiaochun Long, Sachin A. Gupte, Joseph M. Miano

Objective—Unreliable antibodies often hinder the accurate detection of an endogenous protein, and this is particularly true for the cardiac and smooth muscle cofactor, MYOCD (myocardin). Accordingly, the mouse *Myocd* locus was targeted with 2 independent epitope tags for the unambiguous expression, localization, and activity of MYOCD protein.

Approach and Results—3cCRISPR (3-component clustered regularly interspaced short palindromic repeat) was used to engineer a carboxyl-terminal 3×FLAG or 3×HA epitope tag in mouse embryos. Western blotting with antibodies to each tag revealed a MYOCD protein product of ≈150 kDa, a size considerably larger than that reported in virtually all publications. MYOCD protein was most abundant in some adult smooth muscle-containing tissues with surprisingly low-level expression in the heart. Both alleles of *Myocd* are active in aorta because a 2-fold increase in protein was seen in mice homozygous versus heterozygous for FLAG-tagged *Myocd*. ChIP (chromatin immunoprecipitation)–quantitative polymerase chain reaction studies provide proof-of-principle data demonstrating the utility of this mouse line in conducting genome-wide ChIP-seq studies to ascertain the full complement of MYOCD-dependent target genes in vivo. Although FLAG-tagged MYOCD protein was undetectable in sections of adult mouse tissues, low-passaged vascular smooth muscle cells exhibited expected nuclear localization.

Conclusions—This report validates new mouse models for analyzing MYOCD protein expression, localization, and binding activity in vivo and highlights the need for rigorous authentication of antibodies in biomedical research.

Visual Overview—An online [visual overview](#) is available for this article. (*Arterioscler Thromb Vasc Biol.* 2018;38:2184-2190. DOI: 10.1161/ATVBAHA.118.311171.)

Key Words: allele ■ epitope ■ mice ■ muscle, smooth ■ myocardin

The trustworthy detection, localization, and interactive association of a protein are essential in understanding cellular processes under normal and pathological conditions. Yet, biology is plagued by fallacious antibodies,¹ particularly, those directed against transcription factors.² Accordingly, antibodies to a variety of epitope tags have been developed to circumvent the difficulties often encountered with monoclonal or polyclonal antibodies.³ Epitope tagging is commonplace in laboratories using plasmids to study ectopic protein expression. Far fewer examples exist with the tagging of endogenous protein-coding gene loci in mice,^{4–6} likely because of the labor-intensive approach of traditional gene targeting. However, the CRISPR-Cas9 (clustered regularly interspaced short palindromic repeat–associated protein 9) genome-editing system^{7–9} has revolutionized the production of novel mouse strains, including those carrying epitope tags.^{10,11} Here, we present the accurate expression, localization, and binding activity of epitope-tagged MYOCD (myocardin), an SRF (serum response factor) cofactor¹² that powerfully drives the program of vascular smooth muscle cell (VSMC) differentiation.^{13–16}

Materials and Methods

Data available on request from the authors.

Three-Component CRISPR Editing of the *Myocd* Locus

For the *Myocd*^{3×FLAG} mouse, single guide RNA (sgRNA) of sequence ACAGCAGUGGUAACACCCG (synthesized in vitro as described¹⁷) was tested for activity in a split reporter assay¹⁸ (Figure IIB in the [online-only Data Supplement](#)) and injected (50 ng/μl) with *Cas9* mRNA (100 ng/μL; TriLink Biotechnologies) and a symmetrical, single-strand oligonucleotide containing the 3×FLAG sequence (100 ng/μL; Ultramer PAGE-purified; Integrated DNA Technologies) into the pronucleus of C57BL/6J zygotes. The single-strand oligonucleotide was of the same strand as the sgRNA so as to prevent hybridization of the two in the embryo. For the *Myocd*^{3×HA} mouse, synthetic sgRNA (same as above) and CAS9 protein (both from Synthego) were validated for DNA cleavage in an in vitro tube assay as described by the manufacturer. CAS9 protein and sgRNA were mixed (3 pmol each) as a ribonucleoprotein complex and then combined with a 249 single-strand Megamer oligonucleotide (100 ng/μL; Integrated DNA Technologies) before cytoplasmic injection. Viable 2-cell stage embryos were transferred to pseudopregnant C57BL/6J females.

Received on: April 11, 2018; final version accepted on: June 22, 2018.

From the Aab Cardiovascular Research Institute, University of Rochester Medical Center, Rochester, NY (Q.L., Y.H., B.G., M.E.W.-S., C.K.C., Q.Y., O.J.S., J.M.M.); Department of Pharmacology, New York Medical College, Valhalla (V.D., S.A.G.); Department of Cellular and Integrative Physiology, Indiana University School of Medicine, Indianapolis (P.H.); and Department of Molecular and Cellular Physiology, Albany Medical College, NY (X.L.).

The online-only Data Supplement is available with this article at <https://www.ahajournals.org/doi/suppl/10.1161/ATVBAHA.118.311171>.

Correspondence to Joseph M. Miano, PhD, Aab Cardiovascular Research Institute, University of Rochester School of Medicine & Dentistry, 601 Elmwood Ave, Rochester, NY 14624. Email j.m.miano@rochester.edu

© 2018 American Heart Association, Inc.

Arterioscler Thromb Vasc Biol is available at <https://www.ahajournals.org/journal/atvb>

DOI: 10.1161/ATVBAHA.118.311171

Nonstandard Abbreviations and Acronyms

3cCRISPR	3-component CRISPR
Cas9	CRISPR-associated protein 9
CRISPR	clustered regularly interspaced short palindromic repeats
MYOCD	myocardin
qPCR	quantitative polymerase chain reaction
sgRNA	single guide RNA
SRF	serum response factor
VSMC	vascular smooth muscle cell(s)

Local Institutional Animal Care and Use Committees approved all mouse studies.

Mouse Pup Genotyping, Off-Targeting, and Breeding

One-week-old founder pups were toe-clipped or ear-punched, and tissue was digested overnight at 55°C in lysis buffer (50 mmol/L KCl, 10 mmol/L Tris-HCl [pH 9], 0.1% Triton X-100, and 0.2 mg/mL proteinase K) on an interval mixer. The next morning, samples were heated at 95°C for 10 minutes to inactivate the proteinase K and spun down at 15 000g for 10 minutes. Each sample of DNA (1 µL) was mixed with 12 µL nuclease-free water, 10 µL AccuStart II Supermix (Quantabio), and 1 µL each of forward and reverse primers (Table I in the [online-only Data Supplement](#)) flanking the double-strand break (Figure II in the [online-only Data Supplement](#)). Polymerase chain reaction (PCR) conditions were 1 cycle of 95°C for 3 minutes followed by 30 cycles of 95°C (30 s), 58°C (45 s), and 72°C (1 minute) and a final 7-minute cycle at 72°C.

Off-targeting was assessed initially with CCTop,¹⁹ Cas-OFFinder,²⁰ and the MIT CRISPR website²¹ and later with the CRISPOR tool.²² No predicted off-targets were found within 2 megabases of the on-target double-strand break. We selected the top 9 distal off-target sites based on an aggregate analysis of each prediction program. PCR primers flanking each predicted off-target site were synthesized (Integrated DNA Technologies) and used to amplify genomic DNA from founder mice as above only the number of PCR cycles was limited to 28. Each primer pair contained linker sequences positioned at the 5' end of the template-specific primer sequence necessary for next-generation sequencing; the forward primers contained the linker sequence, A C A C T G A C G A C A T G G T T C T A C A, and the reverse primers contained the linker sequence, T A C G G T A G C A G A C T T G G T C T. After the initial 28-cycle PCR reaction, the samples were verified on an agarose gel, and approximately equal amounts were subjected to a second PCR reaction (8 cycles only) using primers containing Illumina adaptor sequence, 10 bp sample-specific barcodes, and the original linker sequences. Amplified sequences were then submitted to the Genomics Core for next-generation sequencing on an Illumina HiSeq 2500 platform. This setup allowed for all 9 amplicons to be sequenced in 1 lane of the sequencer. Raw sequence reads were analyzed for indels with CRISPResso.²³

Positive founder mice derived from CRISPR-Cas9 genome editing are mosaic.^{11,24} We, therefore, backcrossed each positive founder to C57BL/6J mice for Sanger sequencing to confirm germline transmission of each epitope tag. Sanger sequencing of F₁ mice confirmed germline transmission of the correct allele, as well as sequence fidelity in and around the edited region. *Myocd*^{B^{3x}FLAG} was successfully bred through the germline (in 2 founders), and data were similar in both lines. We confirmed 1 mosaic founder carrying the *Myocd*^{B^{3x}HA} tag, but the line was lost because of dystocia of the pregnant founder. We nevertheless isolated tissues for Western (Figure 1B) and limited immunofluorescence microscopy of adult tissues (data not shown). Each of the CRISPR-edited mouse lines is listed in the Major Resources Table in the [online-only Data Supplement](#).

RNA Isolation, Reverse Transcription, and Real-Time qPCR

Total RNAs were isolated using RNeasy Mini Kit (Qiagen, no. 74104) according to the manufacturer's instructions. Reverse transcription was performed using Bio-Rad iScript cDNA synthesis kit (Bio-Rad, no. 1708891) after RNA quantification and DNase I treatment. Real-time quantitative PCR (qPCR) was performed using iTaq Universal SYBR Green Supermix (Bio-Rad, no. 1725121) with customized primers (Table I in the [online-only Data Supplement](#)).

Western Blot

Tissues (from male and female mice, aged 6–10 weeks) were isolated and homogenized in 200 µL of cell lysis buffer (Cell Signaling, no. 9803). After brief centrifugation, supernatants were transferred to fresh 1.5 mL microfuge tubes for protein quantification with DC protein assay kit (Bio-Rad, no. 5000111). Samples were boiled in LDS sampling buffer (Invitrogen, no. NP0007) and subjected to electrophoresis in SDS-PAGE gel. Proteins were transferred to a polyvinylidene difluoride membrane for 2 hours in cold room at 80 V using a Trans-blot machine (Bio-Rad). Membranes were then blocked with 5% nonfat milk in TBS-T (Tris-buffered saline containing 0.1% Tween 20) for 1 hour and incubated with primary antibody for 1 hour at room temperature. After washing, secondary antibodies were incubated for 1 hour at room temperature followed by immersion in chemiluminescence substrate (Thermo Fisher, no. 34080) and exposed to X-ray film. A list of antibodies used is provided in the Major Resource Table in the [online-only Data Supplement](#).

Chromatin Immunoprecipitation

At least 5 mouse aortae were isolated and fixed in 10 mL of 4% paraformaldehyde at room temperature for 10 minutes. One mL of 1.25 mol/L glycine was added to stop crosslinking. Aortae were washed twice with 1×PBS and 1 mL of ChIP (chromatin immunoprecipitation) lysis buffer (50 mmol/L Tris-HCl [pH 8.0], 150 mmol/L NaCl, 5 mmol/L EDTA, 0.1% deoxycholate, 1% Triton X-100, and protease inhibitor cocktail) was added. Tissues were then pulse-sonicated (intervals of 10 s pulse for 2 minutes) and centrifuged at 12 000g for 10 minutes at 4°C. Supernatants were collected and transferred to fresh 1.5 mL microfuge tubes. Mouse anti-FLAG antibody (Sigma-Aldrich, no. F3165) and mouse IgG were added to lysate (~500 µL each) respectively and incubated for 2 hours at 4°C. One-hundred microliters of Dynabeads protein G (Thermo Fisher, no. 10003D) were washed twice with 1×PBS and resuspended in the original volume of ChIP lysis buffer for each ChIP reaction. Magnetic beads were mixed with antibody-lysate and incubated for 2 hours at 4°C. After 5 washes with ChIP lysis buffer, samples were treated with proteinase K (10 mg/mL) at 55°C on a thermomixer for 1 hour. DNA was then recovered and purified by boiling with Chelex-100 resin (Bio-Rad, no. 1422822) for downstream assays, (eg, real-time qPCR).

Isolation and Culture of Mouse Aortic Smooth Muscle Cells

We followed a previously published protocol for isolating mouse aortic SMC.²⁵ In brief, for each independent experiment, 3 mouse aortae were isolated and placed into ice-cold Hank's balanced salt solution in a 15 mL conical tube. Aortae were digested with 3 mL of buffer A (10 mg collagenase II, 10 mg soybean trypsin inhibitor in 10 mL Hank's balanced salt solution) at 37°C for 20 minutes. Aortae were then transferred into clean culture dishes loaded with 10 mL buffer B (DMEM/F12 medium with 20% FBS and 1% Pen-Strep, prewarmed to 37°C). The adventitial layer was peeled off using fine forceps, and aortae were transferred into another clean culture dish with 10 mL buffer B. Each aorta was then cut longitudinally, and the intimal layer was scraped with angled blunt forceps to remove endothelial cells. Aortae were cut with fine scissors into 1 to 2 mm pieces and transferred to 1 well of a 6-well culture plate with 3 mL buffer C (3 mL buffer B+67 µL elastase [Worthington, no. LS002279] at 24.8 mg/mL). Tissues were incubated for 15 minutes at 37°C followed by

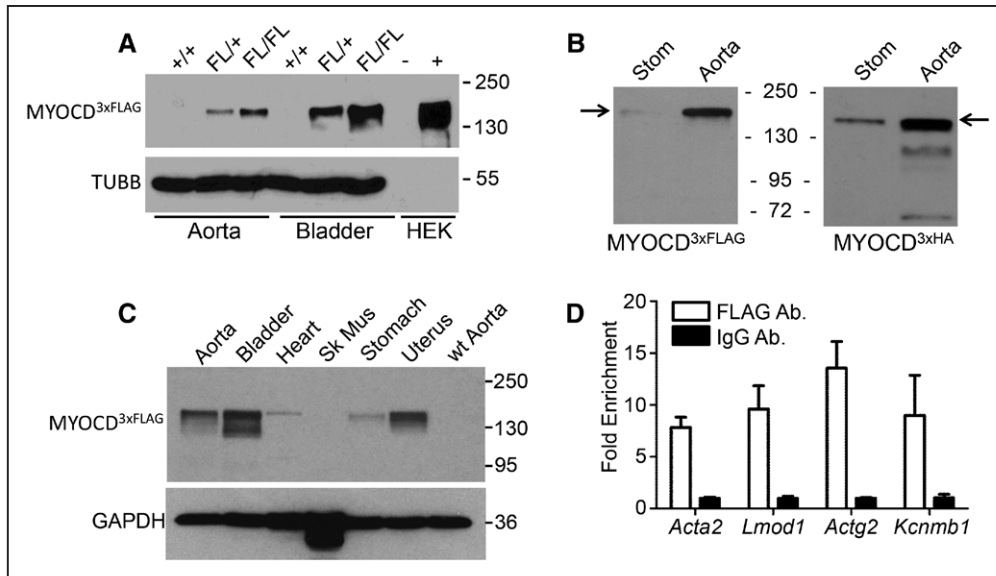


Figure 1. In vivo MYOCD (myocardin) protein expression and binding activity. **A**, Western blot of MYOCD^{3xFLAG} in wild-type (wt; +/+) vs heterozygous and homozygous FLAG (FL)-tagged MYOCD in indicated male mouse tissues. HEK-293 cells untransfected (–) or transfected (+) with 3xFLAG-tagged v1 isoform of MYOCD served as a control. **B**, Parallel Western blots of MYOCD^{3xFLAG} or MYOCD^{3xHA} tagged tissues. **C**, Tissue profile of MYOCD^{3xFLAG} expression in indicated female tissues. Similar results were seen in several independent experiments during the course of 2 y. **D**, In vivo ChIP (chromatin immunoprecipitation)–quantitative polymerase chain reaction (PCR) in homozygous *Myocd*^{3xFLAG} aortae for the indicated target genes using FLAG or IgG control antibodies (Ab). Data are expressed as fold enrichment of FLAG sequence over IgG control. All results were confirmed in at least 1 independent experiment. Data passed test for normality and paired *t* test showed significantly increased enrichment of PCR products with the anti-FLAG antibody, *P*<0.01. Sk mus indicates skeletal muscle; Stom, stomach; and TUBB, beta tubulin.

repeated pipetting with cut 1 mL tips to loosen cells. Cells were incubated another 15 minutes at 37°C and dissociated cells were repeat pipetted with uncut 1 mL tip 5 to 6x. The digestion mixture was transferred to a clean 15 mL canonical tube and 3 mL buffer A was added to stop digestion. Samples were centrifuged at 800g for 5 minutes at 4°C to pellet cells. Cells were resuspended in 5 mL buffer A and plated in a well of 6-well plate. Isolated mouse smooth muscle cells were studied on reaching 50% to 70% confluency.

Confocal Microscopy

Mouse aortic smooth muscle cells were cultured on 22x22 mm coverslips in 6-well plates. Cells were fixed with 4% paraformaldehyde for 10 minutes at room temperature. Coverslips were rinsed in 1xPBS twice and cells permeabilized with 1xPBS containing 0.1% Triton X-100 on an ice bath. Cells were blocked with 3% BSA for 20 minutes at room temperature, and anti-FLAG primary antibody (Sigma-Aldrich, no. F1804; 1:100 dilution) was applied at room temperature for 40 minutes. Coverslips were rinsed twice with 1xPBS and cells incubated with fluorescence-conjugated secondary antibodies (1:200) for 40 minutes at room temperature. Cells were then mounted with ProLong Gold anti-fade reagent with DAPI (4',6-diamidino-2-phenylindole, dihydrochloride; Thermo Fisher, no. P36935) and examined with an Olympus IX81 confocal microscope using uniform settings for all conditions.

Flow Cytometry

Aortae derived from the *mTmG/Myh11CreER*^{T2} cross were digested as mentioned above, and freshly dissociated mouse aortic smooth muscle cells were resuspended in PBS and submitted to the University of Rochester Medical Center Flow Cytometry Core. Cells were sorted according to the Tomato (610 nm) or GFP (green fluorescent protein; 510 nm) signal and quantitated as a percentage of total cells stained for GFP or Tomato.

Transfection Assays

Rat aortic smooth muscle cells (A7r5, ATCC CRL-1444) were transfected with either *Myocd* short intervening RNA (si-*Myocd*, catalog

no. SASI_Rn01_00118674, Sigma-Aldrich) or MISSION siRNA Universal Negative Control (si-Scramble, catalog no. SIC001; Sigma-Aldrich). Cells were mixed with DharmaFECT1 transfection reagent (Lipofectamine 2000, catalog no. T2001-02; Dharmacon) in a 1:1 ratio followed by incubation at room temperature for 20 minutes. Cell mixtures were then added to the wells of cell plates followed by incubation for 48 hours at 37°C. After incubation, cells were washed twice with ice-cold PBS, scraped, and collected in either NP-40 lysis buffer (50 mmol/L Tris-HCl [pH 7.4], 150 mmol/L NaCl, 0.5% Nonidet P-40) containing EDTA-free complete protease and phosphatase inhibitor (Sigma-Aldrich/Roche) for protein estimation or Qiazol buffer for mRNA measurement. For protein measurement, 20 µg samples were run on SDS-PAGE gels, transferred to nitrocellulose membrane, blocked with 4% nonfat milk, and subsequently incubated with TUBA1A (anti- α -tubulin, catalog no. sc5286; Santa Cruz), or MYOCD (catalog no. ab22073; Abcam), followed by incubation with secondary antibodies and detection using SuperSignal West Pico Chemiluminescent Substrate (catalog no. 34080; Thermo Fisher Scientific) on autoradiography film. For *Myocd* mRNA levels total RNA was extracted from aorta and bladder using a Qiagen miRNeasy kit (catalog no. 217004). Input RNA quality and concentration were measured using a Synergy HT Take3 Microplate Reader (BioTek, Winooski, VT), and cDNA was prepared using SuperScript IV VILO Master Mix (catalog no. 11756500, Invitrogen). qPCR was performed in triplicate using TaqMan Fast Advanced Master Mix (catalog no. 44-445-57) in an Mx3000p Real-Time PCR System (Stratagene, Santa Clara, CA). The primers for *Myocd* (Assay ID no. Rn01786178) were purchased from Thermo Fisher Scientific/TaqMan. Results of mRNA expression were normalized to internal control *Gapdh*, and relative mRNA expression was determined using the $\Delta\Delta C_t$ method.

Nano-Liquid Chromatography-Tandem Mass Spectrometry

Rat aorta, urinary bladder, and A7r5 cells were homogenized and lysed in lysis buffer (50 mmol/L Tris-HCl [pH 7.4], 150 mmol/L NaCl, 0.5% Nonidet P-40) containing EDTA-free complete protease and phosphatase inhibitor (Sigma-Aldrich/Roche). Protein levels were measured using Bradford assays (Bio-Rad), after which 30

μg samples were run on SDS-PAGE gels followed by fixing the gel (50% methanol and 10% acetic acid) for 40 minutes at room temperature and washing for 1 hour. Bands corresponding to 100 kDa were cut and subjected to mass spectrometry analysis. The proteins were eluted and analyzed using liquid chromatography-tandem mass spectrometry (Applied Biomics, Hayward, CA). Nano-liquid chromatography fractionation and matrix-assisted laser desorption ionization-time of flight/time of flight were followed by a standard search of the National Center for Biotechnology Information and SwissProt databases using MASCOT. The ≈ 150 kDa FLAG-tagged MYOCD band from mouse bladder was similarly processed and analyzed.

Statistical Analyses

Primary data were assessed for normality with a Shapiro-Wilk test for equal variance (in case of 1- or 2-way ANOVA), and all datasets displayed normal distributions and variances. Accordingly, we used parametric paired t test for comparisons between experimental and control conditions or 1- and 2-way ANOVA for multiple group comparisons. All data analysis was performed in GraphPad Prism 7. Results are expressed as mean \pm SD. A value of $P < 0.05$ was considered statistically significant. For mendelian inheritance of different alleles we used a χ^2 test.

Results

In Vivo MYOCD Protein Expression and Binding Activity

There are at least 4 MYOCD isoforms with predicted molecular weights of 106 kDa (v1, 983 amino acids), 101 kDa (v2, 935 amino acids), 97 kDa (v3, 904 amino acids), and 92 kDa (v4, 856 amino acid).^{26,27} Most commercial antibodies report endogenous MYOCD protein of ≈ 100 kDa, consistent with the predicted molecular weights of each isoform. However, on knockdown of *Myocd* mRNA, there was no corresponding change in a widely assumed MYOCD protein band in A7r5 SMC, mouse and rat aorta and bladder, mouse aortic SMC, and human coronary artery SMC (Figure 1B in the [online-only Data Supplement](#) and data not shown). Similar results were found using a different siRNA to *Myocd* in mouse aortic smooth muscle cell (Figure 1C in the [online-only Data Supplement](#)). Mass spectrometry of the excised 100 kDa bands from rat aorta and bladder, as well as the A7r5 SMC line, revealed no evidence of MYOCD peptides (Table II in the [online-only Data Supplement](#)). Thus, although many commercial antibodies are able to reveal ectopic MYOCD expression (not shown), there is a question as to the accuracy of detecting the endogenous MYOCD protein.

Accordingly, 3-component CRISPR¹¹ was used to target the last coding exon of *Myocd* with either 3 \times FLAG or 3 \times HA epitope tags (Figure 1IA in the [online-only Data Supplement](#)). Correct targeting was validated by Sanger sequencing in 3 \times FLAG (4/35), and 3 \times HA (1/6) founders with no predicted off-targeting in linkage disequilibrium with the on-target site; sequence analysis of the top 9 predicted distal off-target sites showed no mutations, consistent with the high specificity of the sgRNA (data not shown). The *Myocd*^{3 \times FLAG} allele was bred through the germline, and sibling-matings revealed an expected mendelian ratio (Figure 1ID in the [online-only Data Supplement](#)). Western blotting supported biallelic expression of the *Myocd* gene (Figure 1A). The estimated molecular weight of FLAG-tagged MYOCD was ≈ 150 kDa, a size considerably larger than that reported in the literature; *Myocd*^{3 \times HA} mice showed a similar sized band (Figure 1B). An independently

generated *Myocd*^{myc-HA} mouse also revealed MYOCD to have a molecular mass of ≈ 150 kDa (Figure 1IIA in the [online-only Data Supplement](#)). Adult tissue profiling showed the highest expression of MYOCD in bladder and uterus with moderate levels in the aorta; surprisingly lower levels of MYOCD protein were consistently seen in the adult heart (Figure 1C and Figure 1IIB in the [online-only Data Supplement](#)). Importantly, mass spectrometry analysis of the 150 kDa band revealed small quantities of MYOCD protein (Table III in the [online-only Data Supplement](#)). ChIP-qPCR of *Myocd*^{3 \times FLAG} aortic tissue showed significant enrichment of SRF-binding CArG sequences around several known targets of the SRF-MYOCD transcriptional switch (Figure 1D). Despite repeated efforts under numerous experimental conditions, no consistent MYOCD signal was obtained on tissue sections with an array of antibodies to FLAG (data not shown). These in vivo findings reveal a higher molecular weight of MYOCD than previously reported and define, for the first time, reliable detection of endogenous MYOCD protein expression and binding activity in adult mouse tissues.

In Vitro MYOCD Protein Expression

The mTmG reporter mouse²⁸ was crossed with the *Myh11*CreER^{T2} mouse²⁹ to indelibly mark VSMC of the aortic wall with GFP. Most aortic cells from passage numbers 1 to 4 are GFP+; however, beginning at passage number 5 a notable decrease in GFP+ VSMC was seen (Figure 1V in the [online-only Data Supplement](#)). Thus, in vitro studies were restricted to cultures of mouse VSMC at passage 1 to 3. Homozygous *Myocd*^{3 \times FLAG} VSMC exhibited similar mRNA levels of SRF/MYOCD target genes as in wild-type VSMC, suggesting the FLAG epitope tag did not adversely affect MYOCD activity (Figure 1VA in the [online-only Data Supplement](#)). Western blotting of passage 2 VSMC showed MYOCD protein comparable in size to that seen in tissues, indicating the molecular weight of MYOCD did not change appreciably on culture (Figure 1VB in the [online-only Data Supplement](#)). Immunofluorescence microscopy disclosed nuclear-localized MYOCD in cultured VSMC (Figure 2A). Knockdown of *Myocd* mRNA (Figure 2B) resulted in reduced VSMC FLAG-tagged MYOCD protein expression (Figure 2C and Figure 1VB–1VC in the [online-only Data Supplement](#)); we estimate a reduction of at least 10-fold over si-control treated VSMC (Figure 2D). Collectively, these results authenticate a new mouse model for accurate detection of MYOCD protein in both adult tissues and cultured VSMC.

Discussion

We introduce new *myocd* mouse models wherein epitope tags (3 \times FLAG and 3 \times HA) were used to independently target the last coding exon of the *Myocd* locus. The motivation for generating these mice stems from our long-standing difficulty in assessing endogenous levels of MYOCD protein expression in vivo or in vitro in mouse, human, and rat.³⁰ The initial characterization of the epitope-tagged mice reported here reveals several notable findings. First, the 2-fold increase in MYOCD protein expression of homozygous versus heterozygous *Myocd*^{3 \times FLAG} mice indicates biallelic gene transcription. Second, multiple epitope tags demonstrate the molecular weight of the endogenous MYOCD protein to be much higher (≈ 150 kDa) than formerly

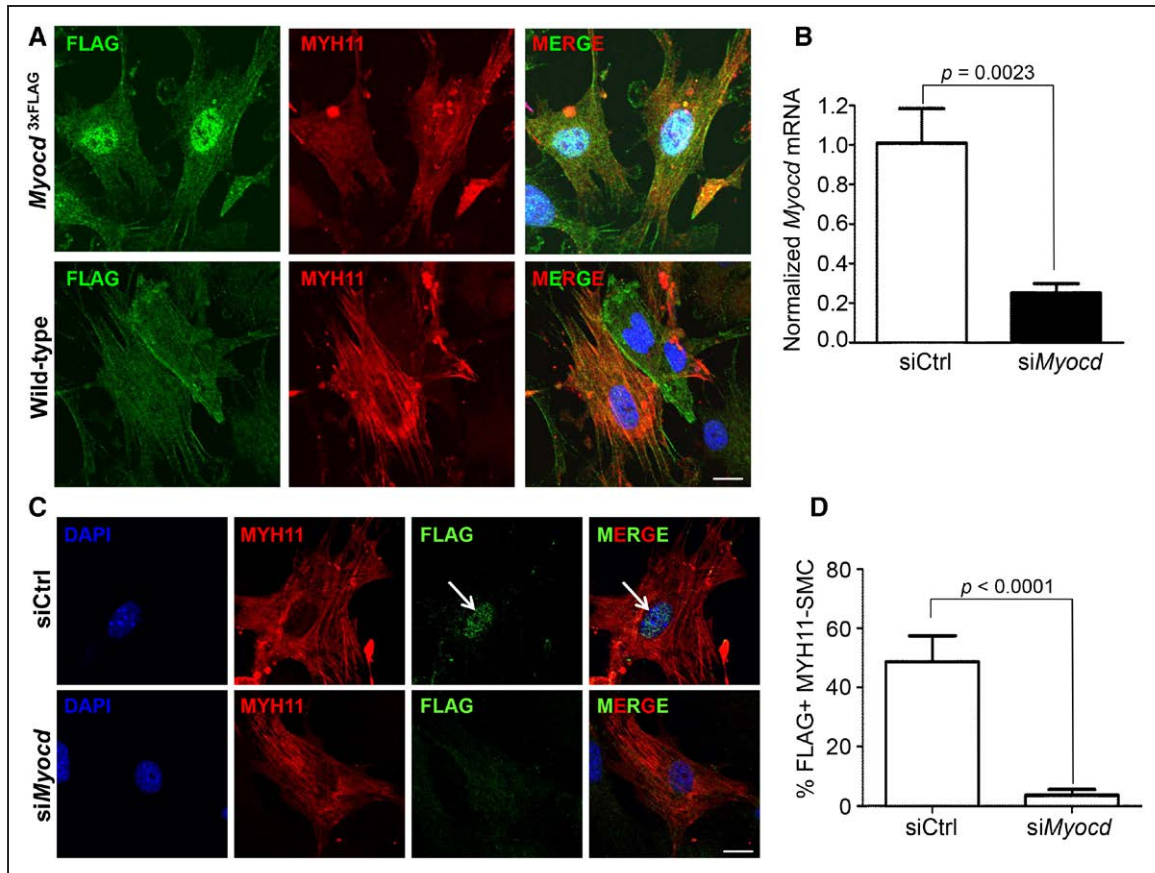


Figure 2. In vitro MYOCD (myocardin) protein expression. **A**, Immunofluorescence microscopy of MYOCD^{3xFLAG} in low-passaged mouse aortic smooth muscle cells (MASMC). Note abundant nuclear staining in Myocd^{3xFLAG} MASMC vs wild-type controls. **B**, Quantitative real-time polymerase chain reaction following siRNA knockdown of Myocd mRNA in cultured MASMC. **C**, Immunofluorescence microscopy of MYOCD^{3xFLAG} in MYH11 positive MASMC treated with si scrambled control (siCtrl, **top**) or siMyocd (**bottom**). Scale bar here and in **A** is 10 μ m. **D**, Quantitative analysis (by 2 independent, blinded investigators) of number of MYOCD-FLAG positive cells costaining for MYH11. See also Figure VC in the [online-only Data Supplement](#). DAPI indicates 4',6'-diamidino-2-phenylindole, dihydrochloride.

reported. Indeed, with rare exception,³¹ the molecular weight of MYOCD protein, when reported, has been between 95 to 105 kDa. We show in data from 2 independent laboratories, using distinct reagents and cell types, that a putative MYOCD protein of \approx 100 kDa does not change with siRNA knockdown of Myocd mRNA. We, therefore, caution investigators using commercial antibodies to MYOCD and urge rigorous analysis to authenticate the specificity of bands so as to avoid further confusion in the field. The higher molecular weight of MYOCD over its predicted size of \approx 100 kDa likely reflects several post-translational modifications shown previously to occur in MYOCD, at least in cultured model systems.^{30,32} Precision CRISPR editing of key amino acids undergoing post-translational modification in the Myocd^{3xFLAG} mouse may clarify the higher-than-expected molecular weight of MYOCD and reveal more nuanced phenotypes than those reported in conditional Myocd knockouts of the heart and vessel wall.^{33,34}

Lower molecular weight bands were seen with FLAG antibodies, particularly in aorta, bladder, and uterus (Figure 1 and Figures III and V in the [online-only Data Supplement](#)). The identity of these bands is unknown at this time, but they could represent different MYOCD isoforms, differential post-translational modifications of a specific MYOCD isoform, or proteolytic cleavage products of MYOCD. The targeting of the C terminus

of MYOCD with epitope tags, as reported here, should allow for the detection and functional assessment, via precision CRISPR editing, of all previously described MYOCD isoforms.^{26,27}

Another noteworthy result was the low-level MYOCD protein in adult heart. This finding was seen in every experiment conducted and cannot be attributed to lower mRNA levels because we originally reported Myocd mRNA to be equivalent in heart and aorta,¹³ a finding we have repeated here (Figure VI in the [online-only Data Supplement](#)). The lower levels of MYOCD protein in adult heart, as compared to bladder and aorta, could reflect a known mechanism of microRNA-mediated repression during cardiac development. Such repression was shown to promote cardiomyocyte maturation while repressing the VSMC gene program.^{35,36} Interestingly, Myocd mRNA is elevated in heart failure,³⁷ a condition characterized by the re-emergence of the fetal heart gene program, which includes an array of VSMC genes. Thus, it seems that levels of MYOCD protein are under exquisite control in the normal adult heart for optimal cardiac function.

The use of a FLAG antibody in ChIP-qPCR studies provides proof-of-principle data supporting ChIP-seq studies in the vessel wall under normal or stress-induced conditions. In this context, a growing number of SRF-independent target genes of MYOCD have been reported.³⁰ The ability to generate mice

in which each *Myocd* allele carries either a 3×FLAG or 3×HA tag offers a rigorous approach to define novel DNA binding sequences and the corresponding DNA-binding transcription factors associated with MYOCD. The mice reported here will also be useful for the discovery of new MYOCD binding proteins or RNAs, especially the class of long noncoding RNA. These and other studies will further illuminate MYOCD biology, thus providing a more integrative understanding of how this cofactor functions under normal and pathological conditions.

In contrast to adult tissues, nuclear-localized MYOCD was observed consistently in cultured VSMC as demonstrated in siRNA knockdown studies. Previous mouse studies showed FLAG-tagged protein expression in tissue sections³⁸ suggesting there may be some steric hindrance in detecting the MYOCD protein in vivo. It is possible the epitope is masked through interactions of MYOCD with other molecules in the cell.^{30,32} However, we have observed consistent staining in adult mouse tissues carrying an inducible HA-tagged *Myocd* transgene (unpublished), and preliminary staining of aorta carrying the *Myocd*^{3×HA} tag suggests that it could be a more discriminating epitope tag than 3×FLAG for immunostaining, though this will require further analysis. Importantly, genetically marked VSMC progressively decrease from culture indicating the need for careful experimental design and circumspect conclusions drawn from in vitro primary VSMC experiments.

The CRISPR revolution has expedited the generation of new mouse models.¹¹ We anticipate similarly tagged mice, as those reported here, will be developed for rigorous protein analyses and accelerated discoveries in vascular biology.

Acknowledgments

We thank Dr Lin Gan and Dr Min Deng of the University of Rochester Genome Editing Resource Facility for their expert RNA and ribonucleoprotein complex microinjections and embryo transfers. We also thank Ms Diane Singer of Albany Medical College for her expert protocol of culturing mouse aortic smooth muscle cells.

Source of Funding

This work was supported by National Institutes of Health grants HL117907 to J.M. Miano; HL132574 (S. Gupte and J.M. Miano); and HL122686 (to X. Long). P. Herring was supported from the Indiana Clinical and Translational Sciences Institute funded in part by UL1TR001108.

Disclosures

None.

References

- Kosmidou C, Efstathiou NE, Hoang MV, Notomi S, Konstantinou EK, Hirano M, Takahashi K, Maidana DE, Tsoka P, Young L, Gragoudas ES, Olsen TW, Morizane Y, Miller JW, Vavvas DG. Issues with the specificity of immunological reagents for NLRP3: implications for age-related macular degeneration. *Sci Rep*. 2018;8:461. doi: 10.1038/s41598-017-17634-1
- Partridge EC, Watkins TA, Mendenhall EM. Every transcription factor deserves its map: Scaling up epitope tagging of proteins to bypass antibody problems. *Bioessays*. 2016;38:801–811. doi: 10.1002/bies.201600028
- Jarvik JW, Telmer CA. Epitope tagging. *Annu Rev Genet*. 1998;32:601–618. doi: 10.1146/annurev.genet.32.1.601
- Chen YI, Maika SD, Stevens SW. Epitope tagging of proteins at the native chromosomal loci of genes in mice and in cultured vertebrate cells. *J Mol Biol*. 2006;361:412–419. doi: 10.1016/j.jmb.2006.06.052

- Lee WJ, Kraus P, Lufkin T. Endogenous tagging of the murine transcription factor Sox5 with hemagglutinin for functional studies. *Transgenic Res*. 2012;21:293–301. doi: 10.1007/s11248-011-9531-9
- Ferrando RE, Newton K, Chu F, Webster JD, French DM. Immunohistochemical detection of FLAG-tagged endogenous proteins in knock-in mice. *J Histochem Cytochem*. 2015;63:244–255. doi: 10.1369/0022155414568101
- Jinek M, Chylinski K, Fonfara I, Hauer M, Doudna JA, Charpentier E. A programmable dual-RNA-guided DNA endonuclease in adaptive bacterial immunity. *Science*. 2012;337:816–821. doi: 10.1126/science.1225829
- Cong L, Ran FA, Cox D, Lin S, Barretto R, Habib N, Hsu PD, Wu X, Jiang W, Marraffini LA, Zhang F. Multiplex genome engineering using CRISPR/Cas systems. *Science*. 2013;339:819–823. doi: 10.1126/science.1231143
- Mali P, Yang L, Esvelt KM, Aach J, Guell M, DiCarlo JE, Norville JE, Church GM. RNA-guided human genome engineering via Cas9. *Science*. 2013;339:823–826. doi: 10.1126/science.1232033
- Yang H, Wang H, Shivalila CS, Cheng AW, Shi L, Jaenisch R. One-step generation of mice carrying reporter and conditional alleles by CRISPR/Cas-mediated genome engineering. *Cell*. 2013;154:1370–1379. doi: 10.1016/j.cell.2013.08.022
- Miano JM, Zhu QM, Lowenstein CJ. A CRISPR path to engineering new genetic mouse models for cardiovascular research. *Arterioscler Thromb Vasc Biol*. 2016;36:1058–1075. doi: 10.1161/ATVBAHA.116.304790
- Wang D, Chang PS, Wang Z, Sutherland L, Richardson JA, Small E, Krieg PA, Olson EN. Activation of cardiac gene expression by myocardin, a transcriptional cofactor for serum response factor. *Cell*. 2001;105:851–862.
- Chen J, Kitchen CM, Streb JW, Miano JM. Myocardin: a component of a molecular switch for smooth muscle differentiation. *J Mol Cell Cardiol*. 2002;34:1345–1356.
- Du KL, Ip HS, Li J, Chen M, Dandre F, Yu W, Lu MM, Owens GK, Parmacek MS. Myocardin is a critical serum response factor cofactor in the transcriptional program regulating smooth muscle cell differentiation. *Mol Cell Biol*. 2003;23:2425–2437.
- Yoshida T, Sinha S, Dandré F, Wamhoff BR, Hoofnagle MH, Kremer BE, Wang DZ, Olson EN, Owens GK. Myocardin is a key regulator of CArG-dependent transcription of multiple smooth muscle marker genes. *Circ Res*. 2003;92:856–864. doi: 10.1161/01.RES.0000068405.49081.09
- Wang Z, Wang DZ, Pipes GC, Olson EN. Myocardin is a master regulator of smooth muscle gene expression. *Proc Natl Acad Sci USA*. 2003;100:7129–7134. doi: 10.1073/pnas.1232341100
- Han Y, Slivano OJ, Christie CK, Cheng AW, Miano JM. CRISPR-Cas9 genome editing of a single regulatory element nearly abolishes target gene expression in mice—brief report. *Arterioscler Thromb Vasc Biol*. 2015;35:312–315. doi: 10.1161/ATVBAHA.114.305017
- Mashiko D, Fujihara Y, Satouh Y, Miyata H, Isotani A, Ikawa M. Generation of mutant mice by pronuclear injection of circular plasmid expressing Cas9 and single guided RNA. *Sci Rep*. 2013;3:3355. doi: 10.1038/srep03355
- Stemmer M, Thumberger T, Del Sol Keyer M, Wittbrodt J, Mateo JL. CCTop: an intuitive, flexible and reliable CRISPR/Cas9 target prediction tool. *PLoS One*. 2015;10:e0124633. doi: 10.1371/journal.pone.0124633
- Bae S, Park J, Kim JS. Cas-OFFinder: a fast and versatile algorithm that searches for potential off-target sites of Cas9 RNA-guided endonucleases. *Bioinformatics*. 2014;30:1473–1475. doi: 10.1093/bioinformatics/btu048
- Hsu PD, Scott DA, Weinstein JA, Ran FA, Konermann S, Agarwala V, Li Y, Fine EJ, Wu X, Shalem O, Cradick TJ, Marraffini LA, Bao G, Zhang F. DNA targeting specificity of RNA-guided Cas9 nucleases. *Nat Biotechnol*. 2013;31:827–832. doi: 10.1038/nbt.2647
- Haessler M, Schöning K, Eckert H, Eschstruth A, Mianné J, Renaud JB, Schneider-Maunoury S, Shkumatava A, Teboul L, Kent J, Joly JS, Concordet JP. Evaluation of off-target and on-target scoring algorithms and integration into the guide RNA selection tool CRISPOR. *Genome Biol*. 2016;17:148. doi: 10.1186/s13059-016-1012-2
- Pinello L, Canver MC, Hoban MD, Orkin SH, Kohn DB, Bauer DE, Yuan GC. Analyzing CRISPR genome-editing experiments with CRISPResso. *Nat Biotechnol*. 2016;34:695–697. doi: 10.1038/nbt.3583
- Yen ST, Zhang M, Deng JM, Usman SJ, Smith CN, Parker-Thornburg J, Swinton PG, Martin JF, Behringer RR. Somatic mosaicism and allele complexity induced by CRISPR/Cas9 RNA injections in mouse zygotes. *Dev Biol*. 2014;393:3–9. doi: 10.1016/j.ydbio.2014.06.017
- Saddouk FZ, Sun LY, Liu YF, Jiang M, Singer DV, Backs J, Van Riper D, Ginnar R, Schwarz JJ, Singer HA. Ca²⁺/calmodulin-dependent protein kinase II- γ (CaMKII γ) negatively regulates vascular smooth muscle cell proliferation and vascular remodeling. *FASEB J*. 2016;30:1051–1064. doi: 10.1096/fj.15-279158

26. Creemers EE, Sutherland LB, Oh J, Barbosa AC, Olson EN. Coactivation of MEF2 by the SAP domain proteins myocardin and MASTR. *Mol Cell*. 2006;23:83–96. doi: 10.1016/j.molcel.2006.05.026
27. Imamura M, Long X, Nanda V, Miano JM. Expression and functional activity of four myocardin isoforms. *Gene*. 2010;464:1–10. doi: 10.1016/j.gene.2010.03.012
28. Muzumdar MD, Tasic B, Miyamichi K, Li L, Luo L. A global double-fluorescent Cre reporter mouse. *Genesis*. 2007;45:593–605. doi: 10.1002/dvg.20335
29. Wirth A, Benyó Z, Lukasova M, Leutgeb B, Wettchüreck N, Gorbey S, Orsy P, Horváth B, Maser-Gluth C, Greiner E, Lemmer B, Schütz G, Gutkind JS, Offermanns S. G12-G13-LARG-mediated signaling in vascular smooth muscle is required for salt-induced hypertension. *Nat Med*. 2008;14:64–68. doi: 10.1038/nm1666
30. Miano JM. Myocardin in biology and disease. *J Biomed Res*. 2015;29:3–19. doi: 10.7555/JBR.29.20140151
31. Morita T, Hayashi K. Arp5 is a key regulator of myocardin in smooth muscle cells. *J Cell Biol*. 2014;204:683–696. doi: 10.1083/jcb.201307158
32. Zheng XL. Myocardin and smooth muscle differentiation. *Arch Biochem Biophys*. 2014;543:48–56. doi: 10.1016/j.abb.2013.12.015
33. Huang J, Cheng L, Li J, Chen M, Zhou D, Lu MM, Proweller A, Epstein JA, Parmacek MS. Myocardin regulates expression of contractile genes in smooth muscle cells and is required for closure of the ductus arteriosus in mice. *J Clin Invest*. 2008;118:515–525. doi: 10.1172/JCI33304
34. Huang J, Min Lu M, Cheng L, Yuan LJ, Zhu X, Stout AL, Chen M, Li J, Parmacek MS. Myocardin is required for cardiomyocyte survival and maintenance of heart function. *Proc Natl Acad Sci USA*. 2009;106:18734–18739. doi: 10.1073/pnas.0910749106
35. Wystub K, Besser J, Bachmann A, Boettger T, Braun T. miR-1/133a clusters cooperatively specify the cardiomyogenic lineage by adjustment of myocardin levels during embryonic heart development. *PLoS Genet*. 2013;9:e1003793. doi: 10.1371/journal.pgen.1003793
36. Heidersbach A, Saxby C, Carver-Moore K, Huang Y, Ang YS, de Jong PJ, Ivey KN, Srivastava D. microRNA-1 regulates sarcomere formation and suppresses smooth muscle gene expression in the mammalian heart. *Elife*. 2013;2:e01323. doi: 10.7554/eLife.01323
37. Torrado M, López E, Centeno A, Medrano C, Castro-Beiras A, Mikhailov AT. Myocardin mRNA is augmented in the failing myocardium: expression profiling in the porcine model and human dilated cardiomyopathy. *J Mol Med (Berl)*. 2003;81:566–577. doi: 10.1007/s00109-003-0470-7
38. Zheng S, Ghitani N, Blackburn JS, Liu JP, Zeitlin SO. A series of N-terminal epitope-tagged Hdh knock-in alleles expressing normal and mutant huntingtin: their application to understanding the effect of increasing the length of normal Huntingtin's polyglutamine stretch on CAG140 mouse model pathogenesis. *Mol Brain*. 2012;5:28. doi: 10.1186/1756-6606-5-28

Highlights

- Nondiscriminating antibodies have hampered the reliable detection of MYOCD (myocardin) protein.
- CRISPR-Cas9 (clustered regularly interspaced short palindromic repeat-associated protein 9) genome editing was used to knock-in epitope tags at the C-terminal end of the *myocd* locus.
- The molecular mass of MYOCD protein is \approx 150 kDa, a size much larger than that reported in the vast literature.
- Epitope tagging of MYOCD allows for facile detection of nuclear MYOCD in cultured cells, as well as associated DNA binding as revealed with ChIP (chromatin immunoprecipitation)-quantitative polymerase chain reaction.
- Epitope tagging of genes with CRISPR affords an unambiguous assessment of protein expression, localization, and associated interactions in the cell.